ELSEVIER

Biochimica et Biophysica Acta 1330 (1997) 233–247

BIOCHIMICA ET BIOPHYSICA ACTA
BBA

Decreased conformational stability of the sarcoplasmic reticulum Ca–ATPase in aged skeletal muscle

Deborah A. Ferrington, Terry E. Jones, Zhihai Qin, Melissa Miller-Schlyer, Thomas C. Squier, Diana J. Bigelow *

Department of Biochemistry, University of Kansas, Lawrence, KS 66045-2106, USA

Received 25 June 1997; accepted 27 June 1997

Abstract

Sarcoplasmic reticulum (SR) membranes purified from young adult (4–6 months) and aged (26–28 months) Fischer 344 male rat skeletal muscle were compared with respect to the functional and structural properties of the Ca–ATPase and its associated lipids. While we find no age-related alterations in (1) expression levels of Ca–ATPase protein, and (2) calcium transport and ATPase activities, the Ca–ATPase isolated from aged muscle exhibits more rapid inactivation during mild (37°C) heat treatment relative to that from young muscle. Saturation-transfer EPR measurements of maleimide spin-labeled Ca–ATPase and parallel measurements of fatty acyl chain dynamics demonstrate that, accompanying heat inactivation, the Ca–ATPase from aged skeletal muscle more readily undergoes self-association to form inactive oligomeric species without initial age-related differences in association state of the protein. Neither age nor heat inactivation results in differences in acyl chain dynamics of the bilayer including those lipids at the lipid–protein interface. Initial rates of tryptic digestion associated with the Ca–ATPase in SR isolated from aged muscle are 16(±2)% higher relative to that from young muscle, indicating more solvent exposure of a portion of the cytoplasmic domain. During heat inactivation these structural differences are amplified as a result of immediate and rapid further unfolding of the Ca–ATPase isolated from aged muscle relative to the delayed unfolding of the Ca–ATPase isolated from young muscle. Thus age-related alterations in the solvent exposure of cytoplasmic peptides of the Ca–ATPase are likely to be critical to the loss of conformational and functional stability. © 1997 Elsevier Science B.V.

Keywords: Aging; Calcium regulation; Sarcoplasmic reticulum Ca–ATPase; Skeletal muscle; Spin label; Fischer 344 rat

1. Introduction

Aging in humans and mammalian models of aging is associated with diminished skeletal muscle performance, such as substantial decreases in the speed of contraction and increases in muscle relaxation times suggesting defects in excitation-contraction coupling [1]. The rate-limiting step of muscle relaxation is mediated by the active transport of calcium across the sarcoplasmic reticulum (SR) membrane by the inte-

Abbreviations: $C_{12}E_9$, polyoxyethylene 9-lauryl ether; EPR, electron paramagnetic resonance; MOPS, 3-(*N*-morpholino) propane-sulfonic acid; SASL, stearic acid spin label; SDS, sodium dodecylsulfate; SDS-PAGE, sodium dodecylsulfate polyacrylamide gel electrophoresis; SR, sarcoplasmic reticulum; ST-EPR, saturation-transfer electron paramagnetic resonance

* Corresponding author. Fax: +1 (913) 864-5321; E-mail: dbigelow@falcon.cc.ukans.edu

PII S0005-2736(97)00158-2

gral membrane protein, the Ca–ATPase. Changes in the SR have been observed in muscle from aged animals; microscopic analysis of muscle sections find decreased surface area of the SR and in chemically skinned fibers, diminished SR volume is observed [1,2]. In isolated SR vesicles, both age-related decreases in calcium transport rates and capacities have been reported, as well as decreased functional stability of the Ca–ATPase when subjected to mild heating [3].

Motivated by these observations, we have used SR vesicles isolated from skeletal muscle of the defined model of mammalian aging, the Fischer 344 rat, to investigate changes in both the function and structure of the SR Ca–ATPase. Our previous work has demonstrated that despite a number of age-related alterations in membrane composition, i.e., phospholipid molecular species, degree of fatty acyl chain unsaturation, and cholesterol content, the physical properties of the bilayer which are critical for Ca–ATPase function remain unchanged [4]. Thus age-related functional changes of the Ca–ATPase most likely result from structural changes of the protein rather than of the SR lipid. In the present study, a thorough characterization reveals virtually no alterations in functional properties of the Ca–ATPase in native SR membranes under optimal assay conditions; however, this protein exhibits a decreased heat stability associated with age. In aged muscle, we find evidence for an altered tertiary structure of the Ca–ATPase from its increased rates of tryptic digestion. At the same time measurements of protein rotational diffusion within the bilayer demonstrate a greater propensity of the Ca–ATPase for irreversible self-association as a result of mild heating.

2. Materials and methods

2.1. Isolation of SR

Native SR vesicles were prepared as described previously [5] with minor modifications [6]. For each preparation, SR membranes were isolated from the hindlimb muscles of equal numbers (2–3 animals per preparation) of young adult (4–6 months, 359 ± 4 g) and aged (26–28 months, 384 ± 12 g) male Fischer strain 344 rats obtained from the National Institute of Aging maintained rat colony (Harlan Sprague Dawley, Indianapolis). SR vesicles were suspended in a medium consisting 0.3 M sucrose and 20 mM MOPS (pH 7.0) and stored at −70°C. Protein concentration was determined using a modified Biuret assay in which 2% Sterox detergent (Bacharach, Pittsburgh, PA) was included to reduce light scattering [7]. Bovine serum albumin was used as the standard. All subsequent analysis were performed using SR membranes from young and aged animals, which were isolated on the same day in order to eliminate variability due to preparation differences.

2.2. Electron microscopy

Native SR vesicles (1.0 mg/ml) were negatively stained with 2% ammonium molybdate (pH 7.3), following the floatation method of Valentine [8]. Specimens were examined using a Joel 1200 Exll transmission electron microscope. Vesicle size was determined from enlarged micrographs with an original magnification of 15,000 times.

2.3. Calcium-dependent ATPase activity

Calcium-dependent ATPase activity was measured at 25°C by colorimetric determination of inorganic phosphate released from vesicles made leaky to calcium by the addition of the calcium ionophore, A23187 [9]. The reaction medium contained 100 mM KCl, 5 mM $MgCl_2$, 4 μM A23187, 25 mM MOPS (pH 7.0), 0.05 mg/ml SR protein, and either 0.1 mM $CaCl_2$ or 1 mM EGTA. The reaction was started by addition of 5 mM ATP and from multiple (four) time points, the initial rate of inorganic phosphate release was used to calculate activity. Activity assayed in the presence of EGTA (basal activity) was subtracted from that assayed in the presence of $CaCl_2$ (total ATPase activity) in order to obtain calcium-dependent ATPase activity. Ionophore stimulation was determined from the ratio of calcium dependent ATPase activities in the presence and absence of the calcium ionophore, A23187.

2.4. Calcium activation measurements

For measurements of ATPase activity at different calcium concentrations, EGTA buffered solutions were used. The assay medium was the same as previously described for calcium-dependent ATPase

activity with the exception that the EGTA concentration was 0.1 mM with the inclusion of sufficient $CaCl_2$ to provide the desired free calcium concentrations. Free calcium concentrations were calculated from total calcium and EGTA concentrations taking into account pH, Mg^{2+}, and nucleotide concentrations [10]. Data was fit to a model for binding to two ligand (calcium) binding sites that explicitly considers the relative affinities and cooperative interactions between the individual ligand binding sites [11]:

$$Y = \frac{K_1[\mathrm{Ca}]_{\mathrm{free}} + 2K_2[\mathrm{Ca}]^2_{\mathrm{free}}}{2(1 + K_1[\mathrm{Ca}]_{\mathrm{free}}) + K_2[\mathrm{Ca}]^2_{\mathrm{free}}},$$

where the macroscopic equilibrium constant K_1 corresponds to the sum of the intrinsic equilibrium constants (k_1 and k_2) associated with calcium binding to the two binding sites on the Ca–ATPase [12]. K_2 represents the equilibrium constant for binding calcium to both binding sites ($k_1k_2k_{12}$), and accounts for any positive or negative cooperativity. Cooperativity may be estimated by assuming that the binding sites have equal intrinsic affinities ($K_1 = k_1 + k_2 = 2K$). Thus the lower limit value of cooperativity (K_c) is given by

$$K_c = 4K_2/K_1^2.$$

2.5. Calcium transport measurements

Calcium uptake was determined by monitoring the time-dependent sequestration of [^{45}Ca] into SR vesicles (0.025 mg ml) in a reaction mixture containing 0.1 M KCl, 5 mM $MgCl_2$, 5 mM oxalate, 25 mM MOPS (pH 7.0), 0.05 mM $CaCl_2$ (including 5 μCi of [^{45}Ca] and 5 mM ATP) [5]. Transported calcium was measured at multiple time points during the reaction by sequentially filtering aliquots of the reaction medium through a 0.45 μm filter and measuring the [^{45}Ca] remaining in the filtrate by scintillation counting. Both initial rates and maximal levels of calcium uptake were calculated from the time dependence of [^{45}Ca] in the filtrate subtracted from total [^{45}Ca].

2.6. Phosphoenzyme formation

Steady-state levels of the phosphorylated enzyme intermediate formed from γ-[^{32}P]–ATP were measured [13]. Phosphorylation was carried out in a reaction mixture containing 80 mM KCl, 5 mM $MgCl_2$, 1 mM EGTA, 20 mM MOPS (pH 7.0), and 0.5 mg/ml protein in the presence and absence of 0.9 mM $CaCl_2$. The reaction was started by addition of 0.1 mM γ-[^{32}P]–ATP (Dupont, N. Billerica, MA) and, after 20 s at 0°C, quenched with 7% trichloroacetic acid (w/v) and 4 mM NaH_2PO_4. The quenched protein was washed four times by repeated centrifugations and resuspensions in 3.5% trichloroacetic acid and 2 mM NaH_2PO_4. The final precipitant was dissolved in 2% SDS, 0.1 N NaOH, 2% Na_2CO_3, and 5 mM NaH_2PO_4. Aliquots were taken from this solution for protein determination [14] and liquid scintillation counting. The calcium-dependent phosphoenzyme intermediate was determined from the difference between values derived from measurements in the presence and absence of $CaCl_2$.

2.7. Phospholipid content

The concentration of phospholipids was measured by assaying inorganic phosphate after ashing and comparing the resulting phospholipid concentration to protein concentration [15].

2.8. Polyacrylamide gel electrophoresis

Sodium dodecyl sulfate polyacrylamide gel electrophoresis (SDS-PAGE) was performed using 7.5% gels, according to the method of Weber–Osborne [16]. Gels were stained for protein with Coomassie blue. The relative abundance of the Ca–ATPase was determined from densitometry of Coomassie blue-stained polyacrylamide gels of SR (Scan Jet IIp, Hewlett-Packard), calculating the percent of the protein band migrating with an apparent molecular weight of 95 kDa relative to all SR proteins present in the samples.

2.9. Heat inactivation

Heat stability of vesicular and micellar SR preparations was determined by monitoring Ca–ATPase activity during incubation of samples at 37°C. The incubation medium contained 5 mM $MgCl_2$, 0.4 mM $CaCl_2$, 20 mM MOPS (pH 7.0), and 1.0 mg/ml pro-

tein. For micellar preparations, 1% polyoxyethylene-9-lauryl ether ($C_{12}E_9$) (Sigma) was included in the incubation medium. For experiments requiring inhibition of proteolysis, the incubation medium included the protease inhibitors aprotinin (76.8 nM), phenylmethylsulfonyl fluoride (0.23 mM), pepstatin A (0.7 μM), leupeptin (1.1 μM), and benzamidine (0.83 mM). For experiments where parallel measurements of Ca–ATPase activity and proteolytic digestion with trypsin were made during heating, the incubation medium contained 5 mM $MgCl_2$, 0.4 mM $CaCl_2$, 50 mM ammonium carbonate (pH 7.2), and SR protein (4 mg/ml).

2.10. Digestion with trypsin

SR protein (5 mg/ml) was incubated at 30°C in a reaction medium containing 50 mM NH_4CO_3 (pH 7.0), 0.1 mM $CaCl_2$ and 1 mM DTT. The digestion was initiated by the addition of trypsin at a ratio of 1 mg of SR protein to 0.02 mg trypsin (SR : trypsin (wt/wt) 50 : 1). At various times after the initiation of the digestion reaction, aliquots were withdrawn and the non-soluble protein was precipitated with trichloroacetic acid (10% (w/v) final concentration), then pelleted by centrifugation ($39{,}000 \times g$) for 15 min. Trichloroacetic acid-soluble peptides were measured from the supernatant with the Lowry protein assay [14] or the more sensitive fluorescamine reaction with free amines [17]. Fluorescence intensity was determined using a Perkin-Elmer spectrofluorometer (λ_{ex} = 390 nm, λ_{em} = 475 nm). The amount of free amine was calculated from a standard curve using glycine as a standard (1–50 μg).

2.11. Spin labeling

Hydrocarbon chain mobility was measured with the fatty acid spin label, a 5-oxyl-4′,4′-dimethyloxazolidine derivative of stearic acid (Aldrich), designated as 5- or 12-stearic acid spin label (5-or 12-SASL), using conventional EPR techniques. The spin label was diluted from a stock solution in dimethylformamide into ethanol before adding to SR at a ratio of less than one spin label per 200 phospholipids, with the final ethanol concentration < 1%. To measure overall rotational motion of the Ca–ATPase protein, the Ca–ATPase was specifically labeled with a short chain maleimide spin label, *N*-(1-oxyl-2,2,6,6-tetramethyl-4-piperidinyl) maleimide (Aldrich) as described previously, permitting a direct measurement of the overall rotational mobility of the Ca–ATPase through the use of saturation-transfer EPR (ST-EPR) [18].

2.12. EPR spectroscopy

EPR spectra were obtained using either a Varian E-109 or Bruker ESP300E spectrometer. Submicrosecond rotational motion of spin labels was detected by conventional EPR (first harmonic absorption in-phase, designated V_1) using 100 kHz field modulation (with peak-to-peak amplitude of 2 G) and a microwave field amplitude of 0.1 G. Submillisecond rotational motion of the maleimide spin-label bound to the Ca–ATPase was detected by saturation-transfer EPR (ST-EPR) (second harmonic absorption out-of-phase, designated V_2'; reviewed by Thomas [19]) using 50 kHz field modulation (with a modulation amplitude of 5 G) and a microwave field intensity of 0.25 G. All EPR samples were suspended in 0.3 M sucrose and 20 mM MOPS (pH 7.0).

2.13. Spectral analysis

The effective rotational correlation times for maleimide spin-labeled Ca–ATPase were determined from ST-EPR spectra using a plot of line shapes versus correlation time based on reference spectra of known correlation time obtained from isotropically tumbling spin-labeled hemoglobin in aqueous glycerol solutions. The relationship between the observed line shape and intensity parameters for this instrument were virtually identical to those previously published [20].

2.14. Statistical analysis

Analyses of data of Table 1 were performed using SR isolated in parallel preparations from young and aged animals testing for statistical significance using a paired *t*-test, with the level of significance set at $p \leq 0.05$. Data are reported as mean ± SEM for all groups. For electron micrographs, the size distribution of vesicles isolated from young and aged animals were evaluated using the Kolmogorov–Smirnov D-

Table 1
Characterization of SR isolated from skeletal muscle of young (4–6 months) and aged (26–28 months) Fischer 344 rats

Characteristic	Mean difference [a]	*n* Pairs	Mean (± SE) values
SR yield	−11 ± 6% [b]	11	1.5 ± 0.2 mg protein/g muscle
Ca^{2+} ATPase abundance [c]	0.1 ± 0.1%	11	36.8 ± 1.6%
Phospholipid content	6 ± 3%	10	0.41 ± 0.01 mg lipid/mg SR
Cholesterol content	13 ± 5% [b]	11	6.2 ± 0.8 mol% of lipid
Phosphoenzyme from ATP [d]	−1 ± 2%	4	3.1 ± 0.4 nmol/mg SR
Calcium-dependent ATPase activity [e]	4 ± 5%	11	2.3 ± 0.2 μmol phosphate/min/mg SR
Calcium-independent ATPase activity [f]	30 ± 10% [b]	11	0.37 ± 0.02 μmol phosphate/min/mg SR
Ionophore stimulation [g]	−7 ± 4%	11	3.6 ± 0.2-fold
Calcium uptake rates	3 ± 8%	3	2.9 ± 0.5 μmol Ca/min/mg SR
Coupling ratio [h]	−1.6%	3	1.22 ± 0.11 Ca/ATP

[a] Difference and SEM, expressed as percentages, between the indicated (*n*) number of paired comparisons of SR membranes isolated from aged relative to those from young muscle. (Positive values indicate age-related increases.) Mean (± SE) values for SR preparations isolated from young animals are indicated in parenthesis.
[b] Statistically different ($\alpha \leq 0.05$) as determined by paired *t*-test.
[c] Determined from densitometry of Coomassie blue-stained gels, calculating the percent of the 95 kDa band relative to the sum of all protein bands.
[d] Enzyme phosphorylation was carried out at 0°C in a reaction medium of 80 mM KCl, 5 mM $MgCl_2$, 1 mM EDTA, 0.9 mM $CaCl_2$, 0.1 μM γ-[^{32}P] ATP, 20 mM MOPS (pH 7.0), and 0.5 mg SR protein/ml.
[e] Calcium-dependent ATPase activity was assayed at 25°C in a medium of 100 mM KCl, 5 mM $MgCl_2$, 0.1 mM $CaCl_2$, 4 μM A23187, 5 mM ATP, 25 mM MOPS (pH 7.0), and 0.05 mg/ml SR protein.
[f] Calcium-independent ATPase activity was assayed as in [e], but using 1 mM EGTA instead of $CaCl_2$.
[g] Ratio of Ca–ATPase activity assayed in the presence and absence of 4 μM A23187.
[h] Ratio of calcium transported per ATP hydrolyzed determined from ratios of calcium uptake and calcium-dependent ATP hydrolysis activities where ATPase activity is assayed in the presence of oxalate and otherwise identical conditions as for uptake activity.

statistic, with the level of significance set at $p \leq 0.05$ [21].

3. Results

3.1. Unaltered membrane ultrastructure and Ca–ATPase expression

SR membranes were purified from the hindlimb skeletal muscles of young adult (4-6 months) and aged (26–28 months) Fischer 344 strain rats. Electron microscopy of negatively stained vesicles was used to evaluate intactness and size of these vesicles. The micrographs demonstrate no gross ultrastructural changes in the isolated SR as a result of age (Fig. 1(A)). The diameters of 210 SR vesicles isolated from either young or aged muscle were measured. The mean diameter (150.8 ± 3.8 nm for young and 151.8 ± 3.4 nm for aged) and size distribution were found to be virtually identical for preparations of SR isolated from young and aged skeletal muscle (Fig. 1(B)). This number of measurements allows detection of at least a 15% difference between the two groups at the 95% confidence level [21]. Dynamic light scattering measurements of these vesicular populations gave comparable results indicating that the size distribution of SR vesicles is not different (data not shown).

Results from the assays of a number of functional and structural properties were compared by paired *t*-tests between SR isolated from young and aged animals in parallel preparations (Table 1). Analysis by paired *t*-test has the advantage of grouping animals which have been exposed to similar environmental conditions (especially, e.g., shipping during different times of the year) which might contribute to variation in preparations. Data was collected for most assays from a total of 48 individual animals, consisting of 11 paired preparations each from young and aged animals. Mean differences between paired comparisons of membranes from young and aged animals are reported, along with the mean values of each assay for SR isolated from young animals. In agree-

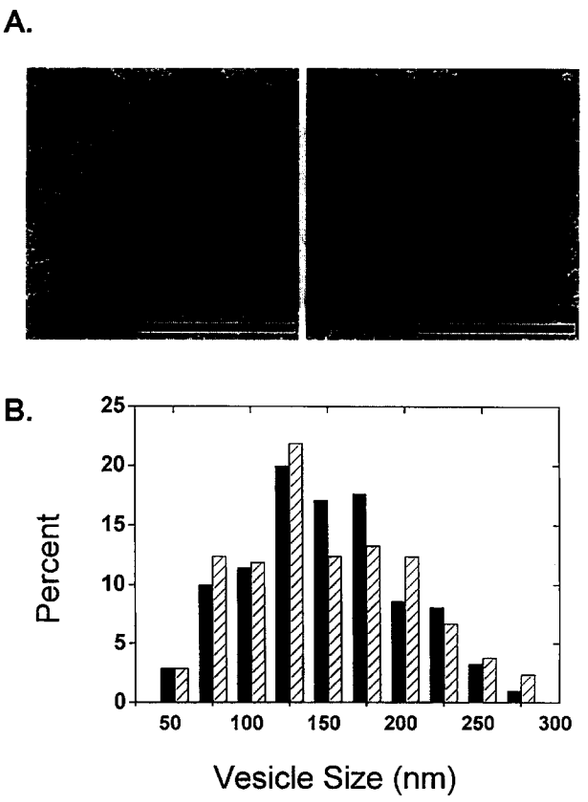

Fig. 1. Panel A: Electron micrographs of negative stained native SR vesicles isolated from skeletal muscle of 5 months old (left) and 28 months old (right) Fischer 344 rats. SR vesicles were negative stained with 2% ammonium molybdate (pH 7.3) and examined with a Joel 1200 Exll transmission electron microscope. Original magnification was 15,000×; bar size represents 500nm. Panel B: Histogram of vesicle size of SR membranes from young (solid) and aged (hatched) skeletal muscle measured from electron micrographs. Vesicle size was determined from enlarged micrographs with an original magnification of 15,000×. Measurement of 210 vesicles in three separate fields were made. The mean vesicle size is 150.8(±3.8)nm and 151.5(±3.4)nm for vesicles of SR preparations from young and aged muscle, respectively.

ment with our previous study characterizing age-related lipid alterations in the SR from a limited number of Fischer 344 rats, we find (i) no significant change in the relative ratio of phospholipids to protein, but (ii) a significant age-related increase (13%) in cholesterol content [4]. Although preparations from aged tissue exhibit a lower yield (11%) of total isolated protein, the relative abundance of the predominant protein, the SR Ca–ATPase, is identical for preparations isolated from young and aged tissue as evidenced by gel densitometry (Table 1). Neither age-related variation in the migration pattern of the Ca–ATPase nor changes in abundance of other SR proteins were observed from SDS polyacrylamide gels. Immunoblots of these gels (not shown) indicate that 8–9% of the Ca–ATPase consists of the slow twitch (SERCA2a) isoform with the remainder consisting of fast twitch (SERCA1) isoform. This isoform composition reflects the fiber type composition of the hind limb muscles [22] and is unaltered by age. In addition, the total amount of functional Ca-ATPase was measured in these SR preparations from steady-state levels of phosphorylated enzyme intermediate (E-P) formed by reaction with γ-[^{32}P]–ATP. The resulting E-P values are virtually identical in SR isolated from parallel preparations of young adult and aged animals (Table 1).

3.2. Functional properties of the Ca–ATPase

Membrane preparations from both young and aged skeletal muscle are enzymatically active and display nearly identical calcium-dependent ATPase activities and calcium transport rates (Table 1). The extent of ionophore stimulation of calcium-dependent ATPase activity indicates that the SR vesicles isolated from both young adult and aged muscle are tightly sealed. Transport efficiency, measured from the ratios of steady-state calcium uptake and ATPase activities occurred with identical stoichiometric coupling ratios (1.2 : 1) for SR from both young and aged skeletal muscle. Although less than the ideal coupling ratio of 2 : 1 measured by transient kinetics, this ratio which is sensitive to specific ligand conditions, has been shown to decrease to much lower values in the steady state [23].

Since calcium-dependent ATPase activity is routinely assayed under saturating calcium concentrations, we also measured the calcium concentration dependence of ATPase activity in order to examine possible differences under more physiological calcium concentrations (Fig. 2). The calcium dependences of the ATPase activity of SR from young and aged skeletal muscle are virtually identical. Fitting the data to a model that explicitly considers the relative affinities and cooperative interactions between individual ligand binding sites results in superimposable curves demonstrating that there are no

age-associated differences in calcium activation and cooperativity.

3.3. Loss of heat stability of the Ca–ATPase

While the initial calcium-dependent ATPase activities of the Ca–ATPase isolated from young and aged muscle are virtually identical, SR isolated from aged muscle is more rapidly inactivated when subjected to elevated temperatures as shown by the time-dependent inactivation observed after prolonged heating at 37°C; activity was subsequently assayed at 25°C (Fig. 3). SR isolated from young muscle exhibits an initial lag time (ca. 2 h), during which the SR is resistant to heat inactivation. Subsequent rapid inactivation occurs with rates that are indistinguishable from the single rapid inactivation rate occurring over the entire time course of heating for SR from aged muscle. Rates of heat-induced inactivation of calcium-independent (basal) ATPase activity are identical for both age groups (data not shown). Proteolysis is minimal during heat inactivation as evidenced by polyacrylamide gels, in which the Ca–ATPase protein band (which migrates with an apparent mass of 95 kDa) remains essentially intact throughout 6 h of heat incubation, during which time significant inactivation has occurred (Fig. 4). After 10 h of incubation at 37°C some loss of Ca–ATPase protein is observed and is accompanied by the accumulation of lower molecular weight proteolytic fragments. Addition of protease inhibitors prevents proteolysis, but does not alter inactivation rates (data not shown).

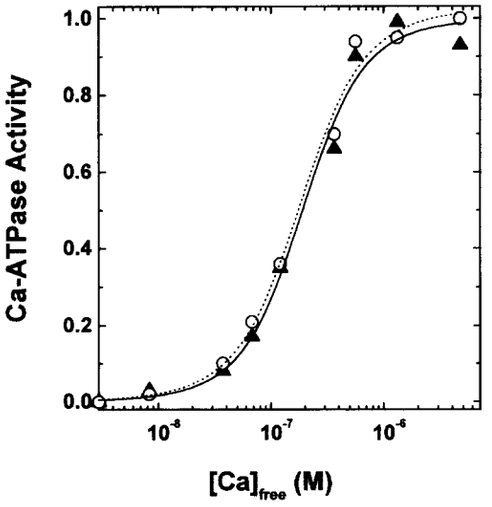

Fig. 2. Calcium concentration-dependence of Ca–ATPase activity of SR isolated from young (○) and aged (▲) skeletal muscle. Activities are normalized relative to the maximal velocities (V_{max} = 2.50(±0.30) and 2.70(±0.26) μmole P_i min^{-1} mg^{-1} for young and aged samples, respectively), and represent means from four separate parallel SR preparations. These data were fit to a model previously described [11] that assumes heterogeneous and cooperative binding for two classes of calcium binding sites. Free energies of binding associated with the equilibrium constant, K_1 (see Methods for details), are −8.8(±0.2) and −8.9(±0.2) kcal/mol; those associated with K_2 are −18.32(±0.09) and −18.53(±0.08) kcal/mol, for SR from young and aged tissues, respectively. Cooperative free energies are −1.5(±0.4) and −1.5(±0.3) kcal/mol for SR from young and aged tissues, respectively. Calcium-dependent ATPase activity was assayed at 25°C, in a medium of 5 mM ATP, 100 mM KCl, 5 mM $MgCl_2$, 4 μM A23187, 0.1 mM EGTA, 25 mM MOPS (pH 7.0), 0.05 mg/ml SR protein and with sufficient calcium to provide the indicated free calcium concentrations.

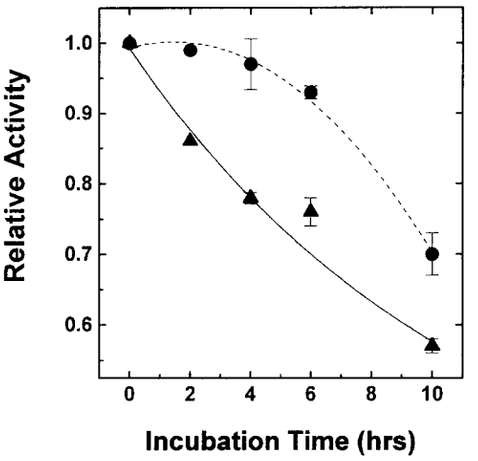

Fig. 3. Heat inactivation during incubation at 37°C of SR vesicles from young (●) and aged (▲) skeletal muscle. Relative activity describes calcium-dependent ATPase activity relative to the initial activity for each sample after various times of incubation in a medium consisting of 1.0 mg/ml protein, 5 mM $MgCl_2$, 0.4 mM $CaCl_2$, 20 mM MOPS (pH 7.0). Aliquots were diluted into a reaction medium containing 0.05 mg SR protein/ml, 100 mM KCl, 5 mM $MgCl_2$, 4 μM A23187, and 25 mM MOPS (pH 7.0) at 25°C for assay of calcium-dependent ATPase activity. Data represents the mean and standard deviation of duplicate activity measurements for one representative experiment. Initial activities were 2.6±0.2 and 2.9±0.1 μmol mg^{-1} min^{-1} for young and aged SR preparations, respectively. Complete inactivation occurred at 22 and 26 h for SR from young and aged muscle, respectively. Comparison of data from several experiments (n = 4) demonstrates that the average rates of rapid inactivation are 0.09±0.05 and 0.05±0.02 h^{-1} for young and aged samples.

The role that the intact membrane plays in the stability of the Ca–ATPase is shown by the experiment in Fig. 5 in which vesicles were solubilized with the nonionic detergent, $C_{12}E_9$. This detergent has been previously shown to support normal enzyme turnover of the SR Ca–ATPase in rabbit fast-twitch skeletal muscle [24]. Similarly, in the case of SR membranes isolated from rat hindlimb skeletal muscle $C_{12}E_9$ solubilization does not inhibit Ca–ATPase activity initially, but dramatically reduces its stability; complete loss of activity occurs within four hours of incubation at 37°C. Rates for this rapid inactivation from preparations derived from young and aged muscle are indistinguishable; the presence of protease inhibitors had no effect on inactivation rates (Fig. 5). Similar results were observed with another nonionic detergent, Triton X-100 (data not shown). These results suggest the possibility that in native SR membranes alterations in lipid–protein or protein–protein interactions, which are primary forces responsible for stabilizing membrane protein structure and activity, may be responsible for the age-related loss of Ca–ATPase stability upon prolonged heating. For example, the SR lipid compositional changes associated with aging [4] may affect either localized or large-scale alterations in bilayer thickness. The concomitant mismatch of lipids with the hydrophobic transmembrane surface of the Ca–ATPase has previously been shown to both inhibit activity and increase self-association of the Ca–ATPase [25,26]. Alternatively, lipid–protein mismatch might result from conformational changes of the protein.

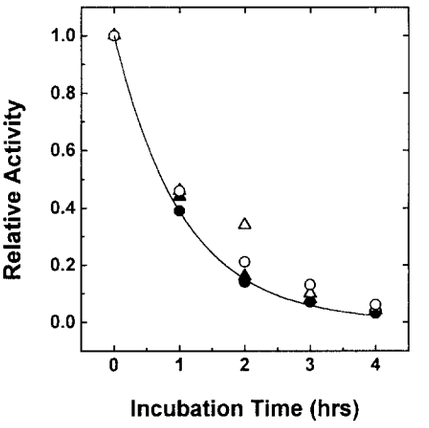

Fig. 5. Normalized calcium-dependent ATPase activity of detergent-solubilized SR during incubation at 37°C. Heat inactivation is shown for SR preparations from young (circles) and aged (triangles) skeletal muscle in the presence (△,○) and absence (▲,●) of protease inhibitors. Incubation conditions were as in Fig. 3, with 1% $C_{12}E_9$ included in the reaction medium. Inactivation for young and aged SR protein were identical. Rates in the presence and absence of protease inhibitors were 0.84(± 0.05)% min^{-1} and 0.90(±0.05)% min^{-1}, respectively.

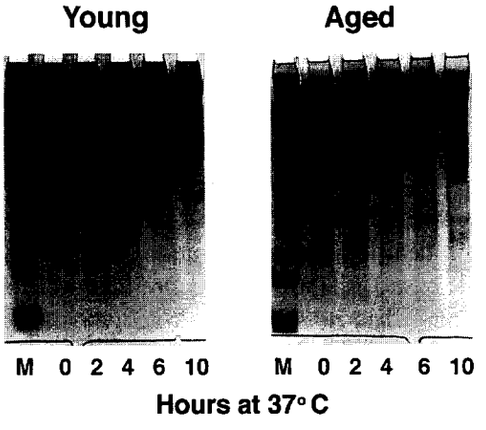

Fig. 4. SR protein composition during incubation at 37°C. SR proteins from young and aged skeletal muscle after incubation for the indicated times (0–10 h) at 37°C were separated (10 μg SR protein/lane) on 7.5% polyacrylamide Weber–Osborne gels subsequently stained with Coomassie blue. Molecular weight markers (lane M) are: myosin (200 kDa), β-galactosidase (116 kDa), phosphorylase B (97 kDa), bovine serum albumin (66 kDa), ovalbumin (45 kDa), carbonic anhydrase (29 kDa), trypsinogen (24 kDa), lysozyme (15 kDa) and aprotinin (6.5 kDa).

3.4. SR lipid fatty acyl chain dynamics

As a means to assess the physical properties of the SR lipid bilayer, fatty acyl chain mobility was monitored using stearic acid spin labels with reporter groups positioned either near the surface (5-SASL) or within the interior (12-SASL) of the bilayer. The spectra of these spin labels in SR membranes display well-resolved extrema, characteristic of anisotropic motion (Fig. 6). These spectra contain contributions from two motional lipid populations, one consisting of lipids which are freely mobile in the bilayer (bulk lipids); the other consisting of a less mobile population of lipids intimately associated with the Ca–ATPase protein (annular or boundary lipids) [27]. Therefore, digital subtractions were used as a means

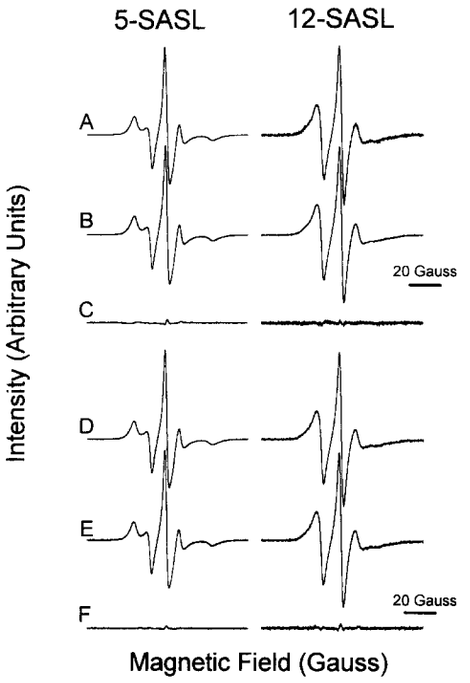

Fig. 6. Conventional EPR spectra of 5-SASL and 12-SASL incorporated into SR membranes isolated from young (A,B) and aged (D,E) skeletal muscle. Spectra were obtained at 4°C in a suspension of 35 mg SR protein/ml, 0.3 M sucrose, 20 mM MOPS (pH 7.0), before (A,D) and after (B,E) incubation at 37°C for 6.5 h. Spectra were recorded with a 100 Gauss scan range. C shows the results of subtracting spectra B from spectra A; F shows the results of subtracting spectra E from spectra D.

to detect any residual spectral shapes indicative of changes in the distribution of bulk or boundary lipids as a result of age or incubation at 37°C. Spectra obtained from heat incubated samples digitally subtracted from those obtained from control samples do not result in a line-shape characteristic of either rapid or slow motion, but rather small and randomly distributed residuals. Thus we find no evidence for alterations in the distribution or mobility of either bulk or boundary lipids as a result of either age or incubation at 37°C. Thus native lipid–protein interactions are maintained with age or heat incubation.

3.5. Ca–ATPase protein dynamics

In order to investigate the possibility that critical elements involving macromolecular interactions in the native SR membrane are modified in an age-dependent manner, spin-label EPR was used to assess Ca–ATPase rotational dynamics in native SR membranes derived from young and aged tissue. The Ca–ATPase was covalently labeled with a maleimide spin label (MSL). The sites of MSL modification have not been identified, but most likely correspond to cysteines 344 and 364, residues that are highly reactive to *N*-ethyl maleimide [28]. Using labeling conditions previously described [18], approximately 9 nmol of spin label per mg SR (i.e., 1.6 mol MSL/mol Ca–ATPase) are bound to the ATPase; these probes are rigidly bound as evidenced by the relatively small population (3–4% of the covalently bound spin labels) of weakly immobilized spin labels (i.e., those probes undergoing nanosecond rotational motion) (Fig. 7). Bound spin labels that are immobi-

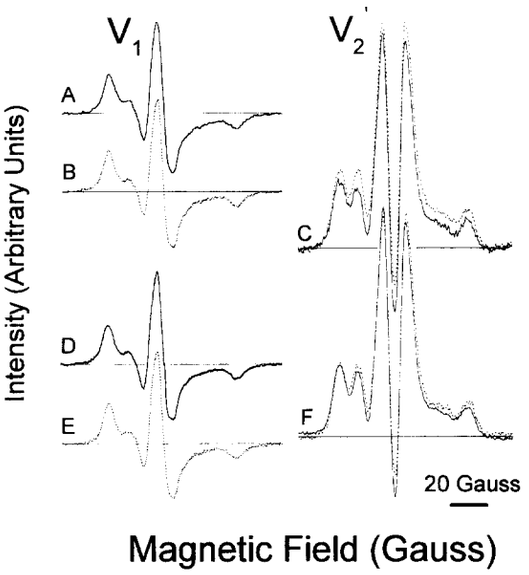

Fig. 7. EPR spectra of maleimide spin-labeled Ca–ATPase in SR isolated from young and aged skeletal muscle. Spectra were measured at 4°C, before (solid line) and after (dashed line) incubation at 37°C for 6.5 h. The V_1 spectra using conventional EPR analysis for Ca–ATPase from aged (A,B) and young (D,E) skeletal muscle demonstrate no difference as a result of heating. The V_2' spectra using ST-EPR of Ca–ATPase from aged (C) and young (F) skeletal muscle exhibit increased spectral intensity as a result of heating, indicative of decreased protein rotational motion. Apparent rotational correlation times calculated from ST-EPR low-field line shapes of these spectra were 90 μs for both young and aged SR before, and 108 and 131 μs for young and aged SR, respectively, after heat incubation. All spectral samples contained 10 mg SR protein/ml in 0.3 M sucrose and 20 mM MOPS (pH 7.0). Spectra were recorded with a 200 Gauss scan range.

lized on the conventional EPR time-scale permit the measurement of the hydrodynamic properties of the Ca–ATPase using ST-EPR. The spectral contribution from weakly immobilized ($\tau_r < 10^{-8}$ s) probes, observable as the second peak in the low-field region of the conventional EPR spectrum, does not change as a result of age or 37°C incubation. In addition, no changes were observed in the low-field line width, a measure of moderately slow (10^{-8} s $\leq \tau_r \leq 10^{-6}$ s) or highly restricted (order parameter ≥ 0.8) motions [29]. Therefore any changes in protein motions detected by ST-EPR are due to changes in slower (microsecond) rotational motion, which provides direct measurement of the hydrodynamic properties of the Ca–ATPase.

Both the line-shape and intensity of the ST-EPR spectrum reflect the protein's motion. In particular, rotational motion serves as a relaxation mechanism, selectively reducing spectral intensity in diagnostic regions of the spectra. Measurements of the rotational dynamics of the Ca–ATPase from SR membranes purified from young and aged skeletal muscle show no initial age-related differences in line-shape or intensity of the ST-EPR spectra (Fig. 7) in agreement with our previous results [4]. However, after incubation at 37°C (and cooling back to 4°C for spectroscopic measurements) spin-labeled Ca–ATPase from both young and aged SR demonstrates increased spectral intensity and associated line-shape changes, indicative of decreased rotational motion (Fig. 8). These spectral changes are particularly apparent in the low- and high-field regions. Effective rotational correlation times were estimated from line-shape changes using reference spectra obtained from spin-labeled hemoglobin (see Section 2). From both the effective rotational correlation times and the spectral changes shown in Fig. 7, it is apparent that the overall protein rotational mobility of the Ca–ATPase decreases during heat treatment for SR from both aged and young muscle, but that the Ca–ATPase from aged tissue exhibits a greater loss of protein mobility for the same time of heating relative to that for protein from young muscle. For example, the Ca–ATPase from aged muscle exhibits a $45 \pm 3\%$ loss of protein rotational mobility after 6.5 h of heat treatment compared to a $12 \pm 8\%$ loss for protein from young muscle. For other times of heat incubation this trend was also observed; samples from aged

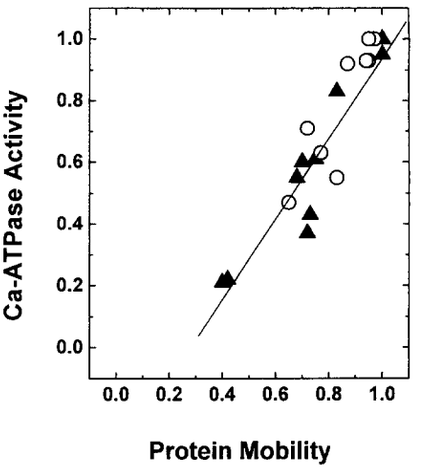

Fig. 8. Correlation between protein rotational mobility of the Ca–ATPase and calcium-dependent ATPase activity in SR membranes isolated from young (circles) and aged (triangles) rat skeletal muscle after various times (0–10 h) of incubation at 37°C. Protein rotational mobility is plotted as the ratio of the correlation time calculated from the low field line shape of a heat incubated sample relative to that of an unheated control sample. Likewise, Ca–ATPase activities of samples are normalized relative to unheated controls. Correlation coefficients between protein rotational mobility and Ca–ATPase activity are 0.88 ± 0.10 and 0.93 ± 0.11 for young and aged samples, respectively.

protein (Fig. 8) showed a greater loss of protein rotational mobility, with an average protein mobility of 0.67 ± 0.06; young samples exhibited an average protein mobility of 0.89 ± 0.03. Despite differential effects of heat treatment on protein mobility, there were identical and good correlations, regardless of age, between the loss of Ca–ATPase mobility and its inactivation ($p = 0.002$) (Fig. 8) consistent with the functional requirement of this protein for a high degree of protein rotational mobility within the plane of the membrane [18,27,30,31].

Since rotational diffusion of a membrane protein is sensitive to both membrane viscosity (i.e., acyl chain dynamics) and the size of the rotating unit within the membrane [32], parallel measurements showing that fatty-acyl spin probe dynamics are unaltered with age or heat incubation (Fig. 6(C) and (F)) allow the observed decreases in Ca–ATPase rotational diffusion to be interpreted in terms of increases in the size of the membrane-spanning domain of the protein. In order to appreciate the magnitude of this change, extrapolation from the data in Fig. 8 indicates that

complete inactivation correlates with an average increase in protein radius of approximately two, suggesting self-association of the Ca–ATPase. This suggestion is supported by previous measurements that demonstrate the same dependence of enzymatic activity on protein rotational mobility when protein mobility was altered by specific chemical crosslinking of Ca–ATPase polypeptide chains [33]. The absence of any SR proteins in amounts stoichiometric to the Ca–ATPase would further rule out the possibility that the observed protein association involves proteins other than the Ca–ATPase. Since the functional unit of the Ca–ATPase has been postulated to be a monomer or dimer [31], complete heat inactivation may correlate with average aggregate sizes as large as tetramers. We note that effective rotational correlation times measured by ST-EPR only allow relative changes to be measured rather than the precise radius of the rotating unit. Moreover, the extent of heterogeneity of the aggregate population, i.e., whether corresponding to discrete oligomeric units or to a distribution of heterogeneous aggregates, cannot be determined from these measurements. Nonetheless, these spin-label EPR measurements indicate that while aging results in no alteration in the average association state of the Ca–ATPase, the protein from aged muscle is characterized by an increased propensity for self-association when subjected to mild heating. That these heat-induced structural alterations persist after cooling to 4°C for spectroscopic measurements indicate that self-association is irreversible.

3.6. Proteolytic digestion of the Ca–ATPase

As a means to probe possible age-related changes in the tertiary structure of the Ca–ATPase that may result in its decreased heat stability, we measured the sensitivity of the Ca–ATPase to tryptic digestion. Of the numerous proteins present in isolated SR, the Ca–ATPase is selectively sensitive to tryptic digestion [34]. When rapid proteolysis of the SR is initiated by exposure to relatively high amounts of trypsin (trypsin : SR ratios (wt/wt) of 1 : 50), cytoplasmically derived peptides are generated that remain in the supernatant after centrifugation of vesicles. Initial rates of proteolysis were evaluated from the measurement of supernatant protein or fluorescent amines (see Section 2). Measurements of eight different

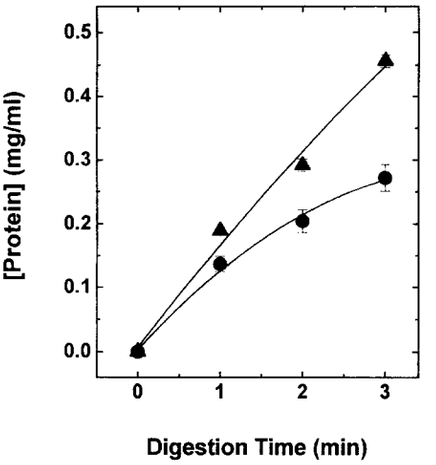

Fig. 9. Tryptic digestion of SR membranes isolated from young (●) and aged (▲) muscles. SR was exposed to rapid tryptic digestion (trypsin : SR (wt/wt) 1 : 50) at 30°C in 50 mM NH_4CO_3 (pH 7.0), 0.1 mM $CaCl_2$ and 1 mM DTT. At various times of incubation, the digestion was stopped with the addition of trichloroacetic acid (10% final concentration) and the concentration of soluble peptides was assayed.

paired preparations demonstrate that the initial rate of proteolysis is $16 \pm 2\%$ more rapid in SR from aged animals ($p = 0.003$) (Fig. 9). These rate differences are consistently observed during the initial release of peptides, involving the proteolytic digestion of approximately 10% of the total protein. Further tryptic digestion occurs at comparable rates for SR isolated from young and aged tissue. Thus the age-related increased proteolytic sensitivity for a small fraction of the 93 cytoplasm tryptic sites of the Ca–ATPase suggests an increase in exposure (unfolding) of a localized region of the protein. Further evidence for this suggestion comes from the unchanged nanosecond motion of the bound maleimide spin label (Fig. 7); global protein unfolding would be expected to result in more rapid nanosecond motion of the maleimide probe detectable by conventional EPR.

Upon heat incubation the differences in initial rates of tryptic digestion are amplified, suggesting further unfolding of a portion of the cytoplasmic domain of the Ca–ATPase (Fig. 10). The time course of changes in initial rates of tryptic digestion for the SR Ca–ATPase from young muscle is biphasic; during the initial 2 h of heat incubation there is either no change or a small decrease in tryptic susceptibility before the subsequent onset of rapid increases in rates of tryptic

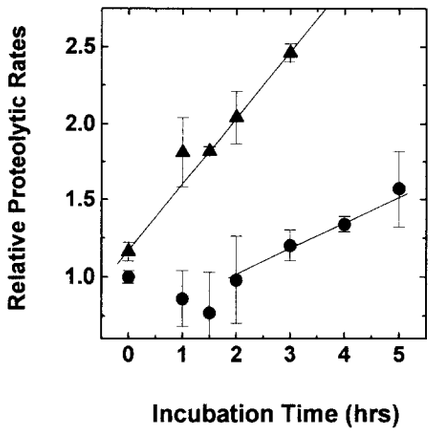

Fig. 10. Initial rates of tryptic digestion of SR membranes from young (●) and aged (▲) muscle after various times of incubation at 37°C. Conditions for incubation at 37°C and subsequent trypsin digestion were as outlined in Fig. 9. Initial rates within the first three minutes of tryptic digestion for each sample are normalized relative to the initial rate from unheated SR isolated from young muscle (0.088 mg protein ml^{-1} min^{-1}). Lines represent linear regression of the relative rates of protein unfolding as assessed by the rapid changes in initial tryptic digestion rates correspond to $0.165(\pm 0.021)h^{-1}$ for protein from young muscle and $0.432(\pm 0.015)h^{-1}$ for protein from aged muscle. These rates are statistically different at $p = 0.05$.

digestion. In contrast, the SR Ca–ATPase from aged muscle exhibits immediate and rapid increases in tryptic digestion, at a rate that is over two-fold greater than that of the rapid inactivation step of young samples suggesting more rapid unfolding of protein from aged muscle. All data relating to the tryptic susceptibility of the Ca–ATPase during heat treatment correlates well with Ca–ATPase activity having correlation coefficients of 0.965 ($p = 0.002$) and 0.994 ($p = 0.006$), respectively, for samples from young and aged muscle.

4. Discussion

4.1. Summary of results

In this study, we have identified alterations in Ca–ATPase conformation and characterized the structural basis for the decreased functional stability of the SR Ca–ATPase in aged skeletal muscle. Further, we have been able to rule out, as contributing factors, age-related alterations in protein expression levels and extensive protein modifications that would alter either binding of the Ca–ATPase to SDS or its migration on SDS-PAGE. The observed increase in functional lability exists in the absence of diminished Ca–ATPase function, i.e., calcium transport, ATP hydrolytic activity, and phosphoenzyme formation, as assayed under optimal conditions (Table 1 and Fig. 3). The time-dependent and irreversible loss of activity accompanying heat incubation does not result from proteolysis of the Ca–ATPase as evidenced by (i) the lack of correspondence between the relatively minimal protein fragmentation (Fig. 4) and the early onset of significant heat inactivation in vesicles (Fig. 3), and by (ii) the absence of altered inactivation rates in both vesicles and micelles when proteolysis is curtailed with protease inhibitors. Inactivation in vesicles is accompanied by both decreasing rotational mobility of the Ca–ATPase without altered fatty acyl chain dynamics (Figs. 6 and 7) and increasing initial rates of tryptic digestion (Figs. 9 and 10), indicating self-association and unfolding, respectively, of individual Ca–ATPase polypeptide chains. Both of these structural alterations have been shown to inhibit transport activity of the Ca–ATPase [18,30,35].

However, the Ca–ATPase would appear to exhibit greater sensitivity to small decreases in protein rotational mobility than to unfolding of its native conformation, as evidenced by the observation that Ca–ATPase protein from aged muscle exhibits a more solvent exposed conformation relative to that in young tissue without loss of enzymatic activity (Figs. 3 and 9). On the other hand, as observed here, as well as in previous studies, Ca–ATPase function is sensitive to even small changes in lipid and/or protein structure that alter Ca–ATPase rotational mobility [18,27,30,31]. The apparent insensitivity of Ca–ATPase activity to age-related changes in its folding pattern may be related to the observation that proteolytic rates differ only for the tryptic digestion of the initial 10% of the protein, suggesting that only a limited region of the cytoplasmic domain is conformationally altered. Future work should focus on identification of the protein sequence(s) involved in these critical structural alterations.

4.2. Structural changes accompanying inactivation

The age-related structural alterations that are characterized by increased tryptic susceptibility may be

responsible for the rapid and immediate inactivation observed for the Ca–ATPase in aged skeletal muscle in contrast to the delayed inactivation in SR from young tissue. Increased solvent exposure of specific amino acid sequences within the Ca–ATPase from aged muscle may promote further unfolding of the cytoplasmic domain upon heating. Although exposure of this region alone is not sufficient to promote self-association of the Ca–ATPase, in the absence of heating, further unfolding of the protein structure coupled with an increased collisional rate of Ca–ATPase polypeptide chains within the plane of the membrane may explain the aggregation and loss of enzyme activity. In contrast, for protein from young muscle, the initial 2 h of heat incubation may promote structural transitions that destabilize the protein and overcome the energy barrier to further inactivation. However, while plausible, this model cannot be confirmed due to the inability of these experiments to kinetically resolve these two processes. The good correlation between the loss of protein rotational mobility and unfolding with Ca–ATPase inactivation suggest that both processes play an important role in the observed inactivation.

4.3. Role of lipid structure

In addition to the age-related protein structural alterations, we have previously described a number of small changes in lipid composition of SR from aged muscle [4]. Even small differences may result in significant effects on protein structure and function if the abundance of essential phospholipids directly interacting with the Ca–ATPase is altered. However, the Ca–ATPase has shown neither a functional requirement nor different binding affinities for any particular phospholipids with respect to headgroup structure or fatty acyl chain unsaturation [36,37]. Consistent with these results we have observed no effect on the fatty acyl chain dynamics of both bulk and protein-associated lipids as a result of age [4]. In the present study, we also observe that these changes have no effect on lipid dynamics after heating (Fig. 6). Thus the possibility that either age or heating results in the accumulation of lipid peroxides can be ruled out since these have been shown to result in marked disordering of the lipid bilayer [38]. Another critical aspect of lipid–protein interactions, not previously considered, involves mismatch between the hydrophobic surface of membrane-spanning proteins and lipid fatty acyl chains as a result of altered bilayer thickness. Model studies have demonstrated that such lipid–protein mismatch has little effect on lipid dynamics, but that even as little mismatch as two carbons in fatty acyl chain length results in substantial Ca–ATPase aggregation [26]. The lack of increased Ca–ATPase association in aged muscle before heating suggests that the observed age-related changes in lipid composition of SR membranes do not contribute to significant changes in bilayer thickness at the lipid–protein interface. Rather, these compositional changes which accompany aging are likely to be largely compensatory in order to maintain the bilayer fluidity and Ca–ATPase rotational mobility that provides optimal calcium transport activity.

4.4. Physiological relevance

From the present experiment using SR membranes derived from a mixture of fast- and slow-twitch fibers characteristics specific to the 8–9% slow twitch (SERCA2a) isoform of the Ca–ATPase cannot be distinguished from those of the predominant fast twitch (SERCA1) isoform. However, experiments with preparations enriched in the slow twitch isoform indicate that this isoform, too, undergoes a loss of heat stability with age (unpublished observations). Thus the conformational features that we have described are likely to be a universal feature of both Ca–ATPase isoforms in skeletal muscle.

The conformational and functional changes in the Ca–ATPase associated with aging are comparable to a number of other proteins from aged tissues which have been previously characterized (reviewed in [39–41]). Proteins from aged tissues have been found to be associated with a variety of defects, including altered expression levels or elevated concentrations of conformationally altered enzymes with diminished enzymatic activity, heat stability, or regulatory properties. These alterations include such post-translational modifications as phosphorylation, acylation, deamidation, glycation, oxidation and covalent cross linking. Of these, we suggest protein oxidation as a possible candidate as an underlying mechanism of this increased heat lability, based on model studies demonstrating the sensitivity of this protein to oxida-

tive modification and the ability of at least one oxidant to simulate increases in both heat lability and proteolytic susceptibility as observed in aging [42–44]. In addition, we have reported the increased accumulation with age of oxidative modifications that result in thiol modification and carbonyl derivatives within the Ca–ATPase [45]. The repair of the latter modifications would require degradation and resynthesis of the modified proteins which has been suggested to be decreased with aging thus resulting in an accumulation of conformationally defective Ca–ATPase proteins in aged muscle [46]. Although cellular conditions are likely to promote greater protein stability than that observed under in vitro conditions, the potential loss of optimal function in vivo, especially in light of the tissue heating that skeletal muscle experiences with even moderate activity (temperatures up to 41–43°C), may contribute to the longer relaxation times observed in skeletal muscle of aged individuals [47,48].

Acknowledgements

We thank Dr. Bruce Cutler for his help in obtaining the electron micrographs and Dr. Jack Schlager for advice on statistical analysis. This work was supported by the Scientific Education Partnership, a Marion Merrell Dow Foundation, the American Federation for Aging Research, and the National Institute of Aging (grant no. AG12275).

References

[1] L. Larsson, G. Salviati, J. Physiol. 419 (1989) 253–264.
[2] W. Decoster, J. DeReuck, G. Sieben, H. VanderEcken, Muscle Nerve 4 (1981) 111–116.
[3] A. Gafni, K.M. Yuh, Mech. Ageing Dev. 49 (1989) 105–117.
[4] A.G. Krainev, D.A. Ferrington, T.D. Williams, T.C. Squier, D.J. Bigelow, Biochim. Biophys. Acta 1235 (1995) 406–418.
[5] J.L. Fernandez, M. Rosemblatt, C. Hidalgo, Biochim. Biophys. Acta 599 (1980) 552–568.
[6] D.A. Ferrington, J.C. Reijneveld, P.R. Bär, D.J. Bigelow, Biochim. Biophys. Acta 1279 (1996) 203–213.
[7] A. Gornal, C. Bardawill, M. David, J. Biol. Chem. 177 (1949) 751–766.
[8] R.C. Valentine, B.M. Shapiro, E.R. Stadtman, Biochemistry 7 (1968) 2143–2152.
[9] P.A. Lanzetta, L.J. Alvarez, P.S. Reinach, O.A. Candia, Anal. Biochem. 100 (1979) 95–97.
[10] A. Fabiato, F. Fabiato, J. Physiol. (Paris) 75 (1979) 463–505.
[11] S. Pedigo, M.A. Shea, Biochemistry 34 (1995) 1179–1196.
[12] G. Inesi, Biophys. J. 66 (1994) 554–560.
[13] H. Barrabin, H.M. Scofano, G. Inesi, Biochemistry 23 (1984) 1542–1548.
[14] O.H. Lowry, N.J. Rosebrough, A.L. Farr, R.J. Randall, J. Biol. Chem. 193 (1951) 265–275.
[15] P.S. Chen, T.Y. Toribara, H. Warner, Anal. Chem. 28 (1956) 1756–1758.
[16] R. Weber, J. Osborne, J. Biol. Chem. 244 (1969) 4406–4412.
[17] A.J. Rivett, Arch. Biochem. Biophys. 243 (1985) 624–632.
[18] S. Negash, L.T. Chen, D.J. Bigelow, T.C. Squier, Biochemistry 35 (1996) 11247–11259.
[19] D.D. Thomas, in: A.N. Martonosi (Ed.), The Enzymes of Biological Membranes, Plenum Press, New York, pp. 287–312
[20] T.C. Squier, D.D. Thomas, Biophys. J. 49 (1986) 937–942.
[21] R.R. Sokal, F.J. Rohlf, in: Biometry, Freeman, New York, 1981.
[22] R.B. Armstrong, R.O. Phelps, Am. J. Anat. 171 (1984) 259–272.
[23] G. Inesi, L. deMeis, J. Biol. Chem. 264 (1989) 5929–5936.
[24] A.J. Murphy, M. Pepitone, S. Highsmith, J. Biol. Chem. 257 (1982) 3551–3554.
[25] A. Johannsson, C.A. Keightley, G.A. Smith, C.D. Richards, T.R. Hesketh, J.C. Metcalfe, J. Biol. Chem. 256 (1981) 1643–1650.
[26] R.L. Cornea, D.D. Thomas, Biochemistry 33 (1994) 2912–2920.
[27] D.D. Thomas, D.J. Bigelow, T.C. Squier, C. Hidalgo, Biophys. J. 37 (1982) 217–225.
[28] K. Saito-Nakatsuka, T. Yamashita, I. Kubota, M. Kawakita, J. Biochem. (Tokyo) 101 (1987) 3365–3376.
[29] R.P. Mason, J.H. Freed, J. Phys. Chem. 78 (1974) 1321–1323.
[30] D.J. Bigelow, D.D. Thomas, J. Biol. Chem. 262 (1987) 13449–13456.
[31] W. Birmachu, D.D. Thomas, Biochemistry 29 (1990) 3904–3914.
[32] P.G. Saffman, M. Delbrück, Proc. Natl. Acad. Sci. USA 72 (1975) 3111–3113.
[33] T.C. Squier, S.E. Hughes, D.D. Thomas, J. Biol. Chem. 263 (1988) 9162–9170.
[34] E. Leberer, J.H.M. Charuk, D.M. Clarke, N.M. Green, E. Zubryzycka-Gaarn, D.H. MacLennan, J. Biol. Chem. 264 (1989) 3484–3493.
[35] I. Jorge-Garcia, D.J. Bigelow, G. Inesi, J.B. Wade, Arch. Biochem. Biophys. 265 (1988) 82–90.
[36] A.G. Lee, K.A. Dalton, R.C. Duggleby, J.M. East, A.P. Starling, Biosci. Rep. 15 (1995) 289–298.
[37] E. London, G.W. Feigenson, Biochemistry 20 (1981) 1939–1948.
[38] J.J.M. van den Berg, J.A.F. Op den Kamp, B.H. Lubin, F.A. Kuypers, Biochemistry 32 (1993) 4962–4967.

[39] E.R. Stadtman, Science 257 (1992) 1220–1224.
[40] M. Rothstein, Mech. Ageing Dev. 9 (1979) 197–202.
[41] A. Gafni, Rev. Biol. Res. Aging 4 (1990) 315–336.
[42] R.I. Viner, A.F.R. Huhmer, D.J. Bigelow, C. Schöneich, Free Rad. Res. 24 (1996) 243–259.
[43] R.I. Viner, D.J. Bigelow, C. Schöneich, Biophys. J. 66 (1994) A120.
[44] D.A. Ferrington, T.E. Jones, R. Viner, K. Thompson, D.J. Bigelow, Biophys. J. 66 (1994) A120.
[45] R.I. Viner, D.A. Ferrington, G.I. Aced, M. Miller-Schlyer, D.J. Bigelow, C. Schöneich, Biochem. Biophys. Acta, in press.
[46] S.I. Rattan, Exp. Gerontol (England) 31 (1996) 33–47.
[47] E. Gutmann, V. Hanzlikova, F. Vyskocil, J. Physiol. 219 (1971) 331–343.
[48] R.H. Fitts, J.P. Troup, F.A. Witzmann, J.O. Holloszy, Mech. Ageing Dev. 27 (1984) 161–172.